Many-electron effects in $L\gamma_{2,3}$ x-ray emission spectroscopy spectrum of BaO

M. Ohno*
Institute of Theoretical Physics, Chalmers University of Technology, S41296 Göteborg, Sweden

R. E. LaVilla
National Institute of Standards and Technology, Gaithersburg, Maryland 20899
(Received 23 May 1988; revised manuscript received 12 September 1988)

The $L\gamma_{2,3}$ ($2s^{-1}\rightarrow 4p^{-1}$) x-ray emission spectrum of BaO was measured in fluorescence with a high-resolution vacuum double-crystal spectrometer. The spectrum was also calculated by the Green's function method. It is shown that the spectrum can be interpreted essentially in terms of a two-level system in the final state, e.g., the $4p$ hole level interacting with the product of the $4p^{-1}\leftrightarrow 4d^{-2}4f$ super Coster-Kronig process. It is also shown that it is necessary to take into account the $4d^{-2}4f$ multiplet.

I. INTRODUCTION

Breakdown of the one-electron picture or in general the quasiparticle picture in the photoionization process from atoms, molecules, and solids has attracted some experimental and theoretical interest[1-10] recently. The most spectacular example is the photoionization of a $4p$ hole of the elements ranging from Pd ($Z=46$) to Yb ($Z=70$) where with a decrease of the atomic number the quasiparticle picture of a $4p$ hole begins to break down.[1,2,4-8] In previous x-ray measurements[8,11] the $L\gamma_{2,3}(2s^{-1}\rightarrow 4p^{-1})$ XES (x-ray emission spectroscopy) spectra of the elements Sn ($Z=50$), Te ($Z=52$), I ($Z=53$), and Xe ($Z=54$) were measured. These XES spectra show the breakdown of the quasiparticle picture of a $4p$ hole due to the strong $4p^{-1}\leftrightarrow 4d^{-2}4(n,\varepsilon)f$ super Coster-Kronig process (configuration interaction).[6-8,11] The overall shape of the XES spectrum is very similar to that of the corresponding $4p$ XPS (x-ray photoelectron spectroscopy) spectrum. The $4p$ XPS spectra measured on solids include the presence of a strong inelastic scattering background which makes a detailed analysis difficult. In contrast, the XES spectrum has a flatter background. In previous works[6,7,11] it was shown that the $L\gamma_{2,3}$ XES spectrum can be interpreted essentially in terms of a $4p$ hole spectral function because of the negligible effect of the initial $2s$ hole on the final $4p$ hole state.

In the present work we measured the $L\gamma_{2,3}$ XES spectrum of BaO using high-resolution x-ray emission spectroscopy and calculated the spectrum by the Green's function method. The observed XES spectrum is very similar to the corresponding Ba $4p$ XPS spectrum. For Ba, the $4p$ ΔSCF hole-energy levels fall below the $4d$ double-hole average ΔSCF energy level (see Table I). In contrast to the case for the elements Pd to Xe where the main ionic excitation strength lies in the continuum, for Ba (Ref. 2) the main ionic excitation strength is concentrated in the $(4d^{-1})_{\rm av}(4d^{-1}4f^{1}P)$ level.[12] Also in contrast to the spectrum of Xe (Ref. 11), there are pronounced satellites near the main line on the low-energy side. Noting the above facts, the spectrum can then be interpreted essentially in terms of a two-level problem, e.g., the $4p$ hole level interacting with the $4d^{-2}4f$ level by the $4p^{-1}\leftrightarrow 4d^{-2}4f$ super Coster-Kronig process. In the case of Ba the screening of the Coulomb interaction between the particle ($4f$ electron) and hole ($4d$ hole) and relaxation of the excited electron ($4f$ electron) becomes very important and must be included within the static relaxation approximation. Furthermore, the multiplet structure of the $4d^{-2}4f$ level must be taken into account. The above-mentioned aspects were neglected in the calculation scheme used for the elements Pd to Xe in previous works[1,6,7] because they were not important.

In the present work, the experimental measurement is of the oxide of barium. However, it is well known that the atom-oxide (or metal) energy shift is fairly level-independent, the atom-oxide energy shifts of the initial ($2s$) and the final ($4p$) holes canceling. Thus we can compare the present atomic calculation with solid-state data. Furthermore, as discussed in previous works,[1-10] the many-body effect (breakdown of the quasiparticle picture in the single-hole excitation) of present interest is the localized atomic process. The present atomic many-body calculation then should be the most suitable approach for the present purpose as demonstrated previously.[1-10]

TABLE I. Energy levels for the ionic excited $4d^{-2}4f$ level of atomic Ba in various approximations and the $4p^{-1}$ levels.

Level	Approximation	Energy (eV)
$4p_{3/2}^{-1}$	ΔSCF	198.0
$4p_{1/2}^{-1}$	ΔSCF	213.5
$(4d^{-2}4f)_{\rm av}$	frozen	180.5
$(4d^{-2}4f)_{\rm av}$	ΔSCF	194.8
$(4d^{-1})_{\rm av}(4d^{-1}4f^{1}P)$	frozen	204.1
$(4d^{-1})_{\rm av}(4d^{-1}4f^{1}P)$	ΔSCF	218.4
$(4d^{-2})_{\rm av}$	ΔSCF	218.7

The overall features of the spectrum are well described by the present Green's function calculation. The present calculation shows that the main line is a well-defined relaxed core level with about half of the original strength of a $4p_{3/2}$ hole level. The satellite nearest to the main line is associated with the $(4d^{-1})_{\rm av}(4d^{-1}4f^1P)_{1/2}$ level [the level split by configuration interaction between the $4p_{1/2}$ hole level and the $(4d^{-1})_{\rm av}(4d^{-1}4f^1P)$ multiplet level]. The broad satellite in the middle is associated with the $(4d^{-1})_{\rm av}(4d^{-1}4f^3D,^3P)_{3/2}$ level. Finally, there is more than half of the original strength of a $4p_{1/2}$ hole level contributing to the continuum.

II. EXPERIMENTAL

The fluorescent Ba $L\gamma_{2,3}$ XES was measured on a vacuum double-crystal spectrometer[13] using Ge (220) crystals ($2d$=4.000 675 Å at 22.5 °C).[14] The sample of reagent grade BaO was finely crushed and dispersed on a 13-μm thick aluminum foil support with an area of 1.5×2.5 cm^2. The BaO sample material was held in place on the supporting foil with a "glue" made of the mixture of benzene and polystyrene of equal volumes. The primary exciting radiation was from a high-power x-ray tube [15] with a cobalt-plated copper anode operating at 13 kV, 190 mA. The monochromatized radiation from the Ba sample was detected with a gas flow proportional counter filled with P-10 (90% argon, 10% methane) at a pressure of 0.92 kPa (700 Torr). The spectrum was obtained by stepscanning the second crystal. The dwell time was 7.5 min/point with a count rate of 0.6 counts/sec at the peak. The experimental spectrum is the average of six scans. Corrections[16] for crystal temperature, vertical divergence, and index of refraction were applied to determine the Bragg angle. The uncertainty of the experimental energy scale of ±0.04 eV is primarily due to counting statistics and modeling of the spectral lines. The Ba $L\gamma_{2,3}$ peak position is 5810.1 ± 0.2 eV, with a full width at half maximum (FWHM) of 5.8 ± 0.4 eV. The diffraction profile had a FWHM of 0.50 ± 0.03 eV.

III. THEORY

In previous works[7,17] it was shown that when one neglects the influence of the initial hole state (i) on the final hole state (f), one obtains the following expression for the x-ray emission process $i^{-1}\rightarrow f^{-1}+\hbar\omega$ by treating the primary ionization and the secondary-emission processes as a single one-step process.

$$I^x(\omega)\propto\omega^3\int dE|\langle i|Z|\varepsilon\rangle|^2\frac{\pi|g_{if}(\omega)|^2}{{\rm Im}\Sigma_i(E)}A_i(E)A_f(E+\omega)\ . \tag{1}$$

Here Z is the dipole moment operator, ω is the photon energy, E is the energy of the initial hole i, ${\rm Im}\Sigma_i$ is the imaginary part of the self-energy of the initial hole i, ε is the kinetic energy of the primary photoelectron, g_{if} is the coupling strength for the electron-photon interaction which is given in the dipole approximation by

$$g_{if}=\langle i|r\cos\theta|f\rangle\ , \tag{2}$$

and $A_i(E)$ is the spectral function of the hole i which is given by

$$A_i(E)=\frac{1}{\pi}{\rm Im}G_i(E)\ . \tag{3}$$

The Green's function $G_i(E)$ of the hole i is given by

$$G_i(E)=[E-E_i^0-\Sigma_i(E)]^{-1}\ , \tag{4}$$

where E_i^0 is the unperturbed hole energy of hole i (Koopman's energy). The self energy of the i hole $\Sigma_i(E)$ consists of the nonradiative part and the radiative part. We consider here only the renormalization of the nonradiative part of the self-energy which is to second order given by

$$\Sigma_i(E)=\sum_{m,j,k}\frac{|\langle im|1/r_{12}|jk\rangle|^2}{E_m^0-E_j^0-E_k^0+E-i\delta}\ . \tag{5}$$

The self-energy $\Sigma_i(E)$ can be divided into two parts corresponding to "static" relaxation and "dynamic" relaxation.[1] Since we are not going to consider any monopole shake-up or shake-off structure, we approximate the static relaxation part of the self-energy by the monopole relaxation energy shift.[1] We renormalize the dynamic relaxation self-energy by approximating the effective three-body [one particle (p)–two holes (h) phh] interaction $I^{phh}(E)$ by the sum of the effective two-body interactions $I^{ph}(E)$ and $I^{hh}(E)$ and neglecting the true three-body interaction which is small. The dynamic relaxation (DR) self-energy is now offered in the form

$$\Sigma_i^{\rm DR}(E)=\sum_{m,j,k}\frac{U_{jkim}\Gamma_{imjk}(E)}{E_m^0-E_{jk}(E)+E-i\delta}\ , \tag{6}$$

$$\Gamma_{imjk}(E)=U_{imjk}+\sum_{m'}\frac{[I^{ph}_{jmjm'}(E)+I^{ph}_{kmkm'}(E)]\Gamma_{im'jk}(E)}{E^0_{m'}-E_{jk}(E)+E-i\delta}\ , \tag{7}$$

$$E_{jk}(E)=E_j(E)+E_k(E)-I^{hh}(E)\ , \tag{8}$$

where we note that U_{jkim} is defined to take into account the important effects of time-reversed diagrams describing Fermi-sea correlation effects. In the present work we solve Eqs. (6) and (7) within the RPAE (random-phase approximation with exchange).[1] The screening of the hole-hole repulsion $I^{hh}(E)$ is calculated in the static monopole approximation and the double hole energy $E_{jk}(E)$ is obtained by the Dirac-Hartree-Fock ΔSCF method.

Wendin[2] pointed out that in the case of Ba, the main ionic excitation strength has become concentrated to the $(4d^{-1})_{\rm av}(4d^{-1}4f^{-1}{\rm P})$ level. He suggested that the screening of the Coulomb interaction between the particle ($4f$ electron) and hole ($4d$ hole) and relaxation of the excited electron ($4f$ electron) must be included within the static relaxation approximation (namely, ΔSCF approximation), and at the same time it is necessary to take into account the multiplet structure of the $4d^{-2}4f$ configuration. Here we consider the scheme similar to

that considered by Wendin.[2] The average energy for the double hole (j^{-2}) and one particle (m) is given by

$$E^{\rm av}_{j^{-2}m}(E)=E_m(E)-2I^{ph}_{j^{-1}m}-2E_{j^{-1}}(E)+I^{hh}_{j^{-2}}\ , \tag{9}$$

where j^{-1} is the $4d$ hole and m is the $4f$ excited electron in the present case. Within the static relaxation approximation

$$\begin{aligned}E^{\rm av}_{j^{-2}m}(E)&\simeq E^{\rm av}_{j^{-2}m}(\Delta{\rm SCF})\\&\simeq E^0_m-2I^{ph}_{j^{-1}m}+\Delta m-E^{\rm av}_{j^{-2}}(\Delta{\rm SCF})\ .\end{aligned} \tag{10}$$

Here Δm is the static relaxation energy shift of the excited electron m. When we do not take into account the static relaxation of the excited electron m, the screening of the Coulomb interaction of the hole (j) and the particle (m), then the average energy $E^{\rm av}_{j^{-2}m}$ (frozen) is given by

$$E^{\rm av}_{j^{-2}m}({\rm frozen})=E^0_m-2F^0(j{:}m)-E^{\rm av}_{j^{-2}}(\Delta{\rm SCF})\ . \tag{11}$$

However, when the excited electron m is coupled to the core hole j^{-1} in a ^1P total angular momentum state and the extra second hole is treated as a spectator, contributing only to the spherically symmetric Hartree potential, i.e., $(j^{-1})_{\rm av}(j^{-1}m\,^1P)$ HFV^{N-2} potential, (HF is Hartree-Fock) then the energy of the $(j^{-1})_{\rm av}(j^{-1}m\,^1P)$ level is given by

$$\begin{aligned}&E(j^{-1})_{\rm av}(j^{-1}m\,^1P)({\rm frozen})\\&\quad=E^0_m-\tilde{I}^{ph}_{j^{-1}m}(^1P)-2F^0(j{:}m)-E^{\rm av}_{j^{-2}}(\Delta{\rm SCF})\ .\end{aligned} \tag{12}$$

Here $\tilde{I}^{ph}_{j^{-1}m}$ is the effective particle-hole interaction beyond the bare Coulomb interaction $F^0(j;m)$, which is treated by the TDAE (Tamm-Dancoff approximation with exchange).[1]

Switching on the static relaxation of the excited electron m and the screening of the Coulomb interaction of the hole (j) and the particle (m), the ΔSCF energy of $(j^{-1})_{\rm av}(j^{-1}m\,^1P)$ level is given by

$$\begin{aligned}&E(j^{-1})_{\rm av}(j^{-1}m\,^1P)(\Delta{\rm SCF})\\&\quad\simeq E^0_m-2I^{ph}_{j^{-1}m}+\Delta m-\tilde{I}^{ph}_{j^{-1}m}(^1P)-E^{\rm av}_{j^{-2}}(\Delta{\rm SCF})\\&\quad\simeq E^{\rm av}_{j^{-2}m}(\Delta{\rm SCF})+E(j^{-1})_{\rm av}(j^{-1}m\,^1P)({\rm frozen})\\&\qquad-E^{\rm av}_{j^{-2}m}({\rm frozen})\ .\end{aligned} \tag{13}$$

IV. NUMERICAL PROCEDURE

We discuss briefly the numerical procedure for the evaluation of the Green's function and refer the reader to previous works[1,7] for details.

A. The final 4p hole state

The dipolar fluctuation process involves correlation between angular distortions of atomic shells, where the $4p$ core hole and $4d$ charge densities correlate with each other by nonspherical dipolar distortions of the $4p$ and $4d$ charge densities. In the case of a $4p$ hole for the elements around Xe, this dipolar coupling is extremely strong.[1,2,6] In the present work we shall be particularly interested in the $4p^{-1}\leftrightarrow 4d^{-2}n(\varepsilon)f$ super Coster-Kronig processes, and the $4p^{-1}\leftrightarrow 4d^{-1}5s^{-1}\varepsilon p$ and $4p^{-1}\leftrightarrow 4d^{-1}5p^{-1}\varepsilon d$ Coster-Kronig processes. We have used the frozen core approximation[1] to evaluate both the real and imaginary part of the dynamic relaxation self-energy given by Eq. (6) in order to consistently treat the decay width and shift of the final $4p$ hole state. For excited (particle) states we use the $(j^{-1})_{\rm av}(k^{-1}m^1P)$ HFV^{N-2} potential constructed by frozen neutral ground-state orbitals.[1] By calculating the discrete and continuum wave functions for the excited electron m in this potential, we include directly a certain selection of the interaction matrix elements in Eq. (7). Using this basis set is the same as working in the TDAE for the $k^{-1}m$ dipole response and including the Hartree potential from the second hole j.[1] The Fermi-sea correlation diagrams can now be expanded through the integral Eq. (8) within the RPAE.

B. The initial 2s hole state

The dynamical relaxation of the initial $2s$ hole is also important. In the case of Xe, the experimental atomic $2s$ hole energy as determined in a previous XES experiment[11] is 5452.2 eV, which is shifted as much as ≈7 eV from the Dirac-Hartree-Fock (DHF) ΔSCF energy.[7,11] The theoretical $2s$ hole-energy calculation of Xe by the Green's function methods is 5452.8 eV in good agreement with experiment.[11] The calculated $2s$ hole-energy shift for Nd ($Z=60$) and Sm ($Z=62$) is 6.6 and 6.7 eV, respectively[11] and for the elements Ag ($Z=47$) to Sb ($Z=51$) the $2s$ hole-energy shift ranges from 6.8 to 8.7 eV.[18] The present work assumed a similar shift for Ba ($Z=56$). Thus we used 5996.6 eV as the $2s$ hole energy (6003.7 eV for DHFΔSCF). We also assumed that the spectral function of the initial $2s$ hole is a Lorentzian profile. The width of the $2s$ hole (3.57 eV) is taken from the theoretical result by Chen *et al.*[19]

C. The energy parameters

For the unperturbed $4p$ level energies [in Eq. (4)], we use the DHFΔSCF energies given in Table I. Also tabulated in Table I are the calculated energy levels for the ionic $4d^{-2}$ and $4d^{-2}4f$ levels of atomic Ba in various approximations discussed in Sec. V. The DHFΔSCF calculation shows that the multiplet structure of the $4d^{-2}$ level ranges from 213.6 to 227.0 eV with an average of 218.7 eV. The $4d^{-2}$ and $4d^{-2}4f$ energy levels tabulated in Table I include the relativistic energy shifts of the $4d$ hole but neglect the relativistic energy shift of the $4f$ electron. We note that the $(4d^{-1})_{\rm av}(4d^{-1}4f^1P)$ level is pushed to the vicinity of the $(4d^{-2})_{\rm av}$ threshold. According to Wendin,[2] the relaxed $(4d^{-2}4f)_{\rm av}$ configuration should be split into two main groups of lines, one around the $(4d^{-1})_{\rm av}(4d^{-1}4f\,^3P,^3D)$ levels and the other around the $(4d^{-1})_{\rm av}(4d^{-1}4f^1P)$ levels. The $^3P,^3D$ parent levels should lie around the configuration average level. For the present calculation we take the average $4d^{-2}4f$ ener-

gy for the ^3P and ^3D parent levels. The RPAE leads to a reduction of the singlet and triplet splitting and pushes the ^1P parent level further below the $4d^{-2}$ threshold to the energy of (15.77 Ry)=214.6 eV.

D. Spectral function

For the final $4p$ hole state, we explicitly calculate the spectral functions for the $4p_{1/2}$ and $4p_{3/2}$ levels and define a statistically weighted spectral function.[1]

V. RESULTS

In Figs. 1–3, we show the experimental and various theoretical $L\gamma_{2,3}$ XES spectra of BaO. Figure 4 is a schematic view of the level splitting of $4p$ hole levels due to strong configuration interaction between a $4p^{-1}$ level and the $4d^{-2}4f$ level within the framework of the several approximations used in this report. Note that the $4d^{-2}4f$ levels plotted in Fig. 4 are shifted from the values listed in Table I due to the ground-state correlation introduced by RPAE.

A. Approximation A

The spectrum A (Fig. 1) is obtained by using the $(4d^{-1})_{av}(4d^{-1}4f^1P)$ frozen energy level and the $(4d^{-2})_{av}$ ΔSCF threshold energy. The energy of the prominent peak obtained is 5810.5 eV which is in excellent agreement with the experimental one (5809.8 eV). This peak has about $\approx$50% of the original strength of the $4p_{3/2}$ hole level. The calculated XPS energy is 186.1 eV which agrees quite well with the atomic binding energy (186.6 eV) estimated from the solid-state XPS data (178.6 eV) for the metal[20] by adding the atom-solid energy shift ($\approx$8 eV).[21] We consider that the metal-oxide energy shift is very small. The experimental "atomic" $2s$ energy of Ba obtained from the present XES data is 5996.4 eV, which is also in excellent agreement with the estimated atomic $2s$ hole energy 5996.6 eV used in the present calculation. The energy of the satellite nearest to the main line obtained by the present calculation is 5804.5 eV, which is in good agreement with experiment ($\approx$5803 eV). It contains about 30% of the original strength of the $4p_{1/2}$ hole level. It may be reasonable to associate this satellite with the $(4d^{-1})_{av}(4d^{-1}4f^1P)_{1/2}$ level, where the index $\frac{1}{2}$ here means the level originated from a $4p_{1/2}$ hole level. The broad satellite which lies next to this satellite is not reproduced by this calculation. Instead, about 10 eV lower in energy a prominent satellite is obtained ($\approx$5786.5 eV) with about 30% of the original $4p_{3/2}$ hole-level strength. The remainder of the original strength of $4p_{3/2}$ (about 20%) and $4p_{1/2}$ ($\approx$70%) goes to the continuum.

B. Approximation B

The theoretical spectrum marked by B (Fig. 1) is obtained by taking only the $(4d^{-1})_{av}(4d^{-1}4f^1P)$ (ΔSCF) level into account for the $(4d^{-2}4f)$ multiplet levels. When the spectrum is calculated by using the average

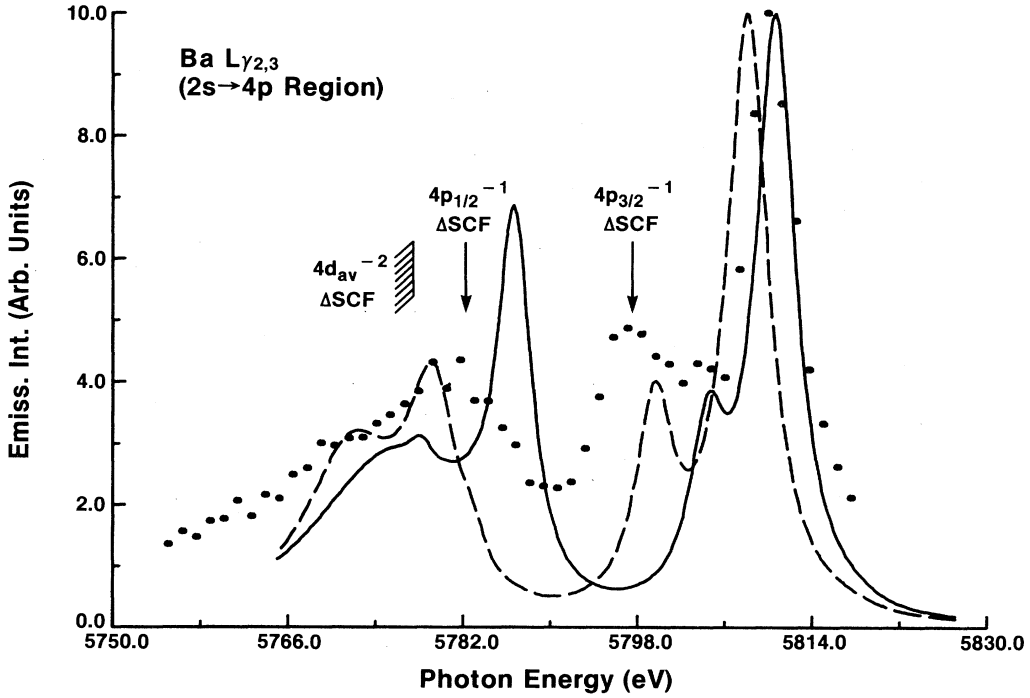

FIG. 1. The x-ray emission of Ba $L\gamma_{2,3}$ ($2s\rightarrow 4p$ region) from BaO. The experimental spectrum is the solid dots. The theoretical spectra are the solid line by approximation A and the dashed line by approximation B. The $4p_{1/2,3/2}$ and $4d^{-2}$ (ΔSCF) XES positions plotted were obtained by using the $2s$ energy of 5996.6 eV.

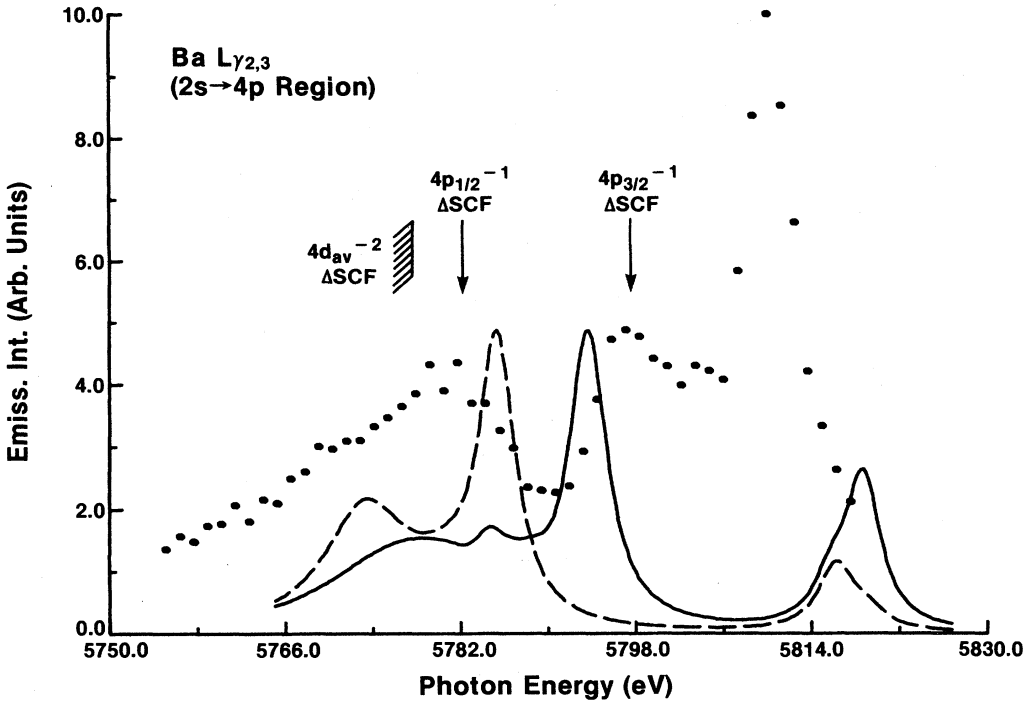

FIG. 2. The x-ray emission of Ba $L\gamma_{2,3}$ ($2s \rightarrow 4p$ region) from BaO. The experimental spectrum is the solid dots. The theoretical spectra are the solid line by approximation C and the dashed line by approximation D. The $4p_{1/2,3/2}$ and $4d^{-2}$ (ΔSCF) XES positions plotted were obtained by using the $2s$ energy of 5996.6 eV.

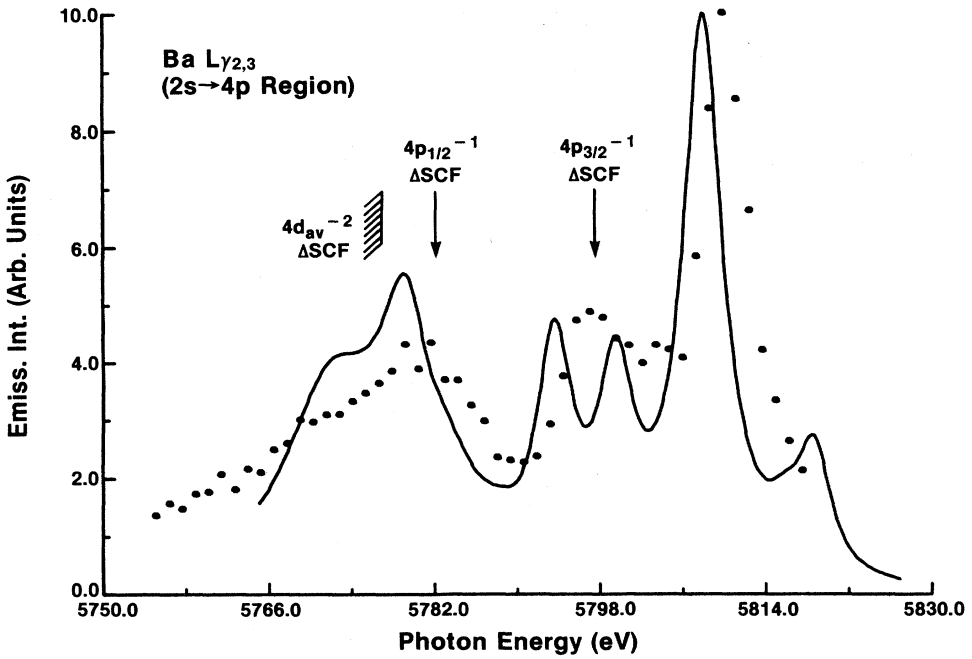

FIG. 3. The x-ray emission of Ba $L\gamma_{2,3}$ ($2s \rightarrow 4p$ region) from BaO. The experimental spectrum is the solid dots. The solid line is the theoretical spectrum $S(E)$ composed of $S(E)$=approximation B+(0.47) approximation C. The $4p_{1/2,3/3}$ and $4d^{-2}$ (ΔSCF) XES positions plotted were obtained by using the $2s$ energy of 5996.6 eV.

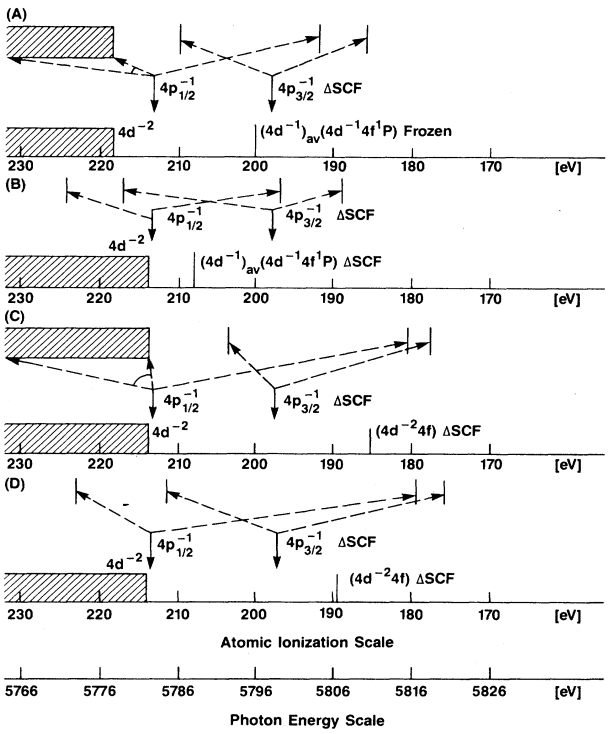

FIG. 4. Schematic diagram displaying the calculated splitting of the $4p$ hole levels due to strong configuration interaction between the $4p$ hole and the $4d^{-2}4f$ multiplet levels. See text for further details.

$4d^{-2}$ (ΔSCF) energy as in the case of spectrum A, the theoretical spectrum is shifted about 5 eV lower in photon energy. Therefore in the following approximations (B,C,D) we used the lowest $4d^{-2}$ ΔSCF energy level (213.6 eV), which is about 5 eV lower than the average $4d^{-2}$ ΔSCF energy as the effective $4d^{-2}$ energy. Note that consequently the multiplet levels as the unperturbed levels are shifted about 5 eV lower from the values listed in Table I. The present result is obtained using this $4d^{-2}$ energy level. The theoretical prominent peak is shifted 2 eV to lower energy (5807.8 eV) from the experimental peak. The calculation shows that this main peak contains about 70% of the original strength of the $4p_{3/2}$ hole level and remains as a well-defined relaxed core level. The satellite nearest to the main line is shifted about 3 eV to lower energy (5799.6 eV) from the experimental first satellite. About 40% of the original strength of the $4p_{1/2}$ hole level remains in this final state as a well-defined relaxed core level. As in the case of spectrum A, it seems reasonable to associate this satellite with the $(4d^{-1})_{av}(4d^{-1}4f^{1}P)_{1/2}$ level. About 30% of the $4p_{3/2}$ hole and 60% of the $4p_{1/2}$ hole levels are spread over the continuum which represents the broad asymmetric peak around the unperturbed $4p_{1/2}$ (ΔSCF) position. Note that the previously mentioned interpretation is based on the calculation which takes into account only the ^{1}P parent level for the $4d^{-2}4f$ multiplet structure.

C. Two kinds of approximations for the $^{3}P, ^{3}D$ parent levels

1. Approximation C.

Using the same basis set used in calculating spectra A and B, we shift the $4d^{-2}4f$ multiplet level energy to the average $4d^{-2}4f$ ΔSCF position to simulate the effects of the $(4d^{-1})_{av}(4d^{-1}4f^{3}P, ^{3}D)$ multiplet level. Note that the multiplet level is shifted further down (as much as ≈ 5 eV) by the ground-state correlation introduced by the RPAE approximation. This is also the case with the calculation of the spectra A and B. The spectrum obtained is labeled by C in Fig. 2.

2. Approximation D

We use the V^{N-2}HF average potential instead of $(4d^{-1})_{av}(4d^{-1}4f^{1}P)V^{N-2}$ HF potential to generate both discrete and continuum wave functions. The multiplet level is shifted to the average $4d^{-2}4f$ ΔSCF position to obtain the spectrum D in Fig. 2. The multiplet level will not be shifted further because we do not introduce the RPAE approximation in this calculation.

Note that the experimental feature around ≈ 5796 eV is well described by this calculation except for an energy shift ≈ 3 eV (5793.6 eV for spectrum C) and 11 eV (5785.2 eV for spectrum D). Both calculations show that this satellite may be associated with the $(4d^{-1})_{av}(4d^{-1}4f^{3}D, ^{3}P)_{3/2}$ level with about 50% of the original strength of the $4p_{3/2}$ hole level. The remaining strength of the $4p_{3/2}$ hole level and $\approx 70\%$ of the $4p_{1/2}$ hole level interacting with the $(4d^{-1})_{av}(4d^{-1}4f^{3}D, ^{3}P)$ level goes to the continuum. The peaks obtained around 5818 eV are probably mathematical fictions and do not correspond to any physical state.

D. Spectrum $S(E)$

The spectrum $S(E)$, Fig. 3, is a weighted linear sum of the $4p$ spectral functions calculated by the same approximation for the singlet and triplet multiplets. The weighting ratios indicate the effective weight of the singlet and triplet multiplets calculated in the present approximation. The correspondence of $S(E)$ with experiment is reasonably good within the limits of this approximation.

VI. DISCUSSIONS

In the present calculation we performed separate calculations for different multiplet levels. In principle, one should calculate the multiplet-level-dependent self-energy, namely, taking into account explicitly the angular momentum coupling of the two-hole–one-particle state and also the particle-hole and hole-hole interactions appropriate to their couplings. This is certainly a very difficult task which is beyond the scope of the present work. When we consider the relative positions of the multiplet levels, the satellite nearest to the main line may be associated with $(4d^{-1})_{av}(4d^{-1}4f^{3}D, ^{3}P)_{1/2}$ as suggested by Wendin.[2] However, the present calculations give fairly good agreement with experiment for the relative position and intensity of the main line and its nearest sa-

tellite when the near satellite is associated with the $(4d^{-1})_{av}(4d^{-1}4f^1P)_{1/2}$ level.

Note that the $(4d^{-1})_{av}(4d^{-1}4f^1P)$ multiplet level lies with the correct weight approximately at the center of gravity of the multiplet structure. Therefore, the spectrum *A* gives a fairly good description of the overall spectral shape in the immediate main line region and continuum.

The present atomic Green's function calculation gives good overall agreement with experiment. This shows that the many-electron effect of present interest is localized on the atomic site. Concerning the energy, we note that the atom-oxide energy shift of the initial and final hole cancels out, as the atom-oxide energy shift is fairly level independent. Furthermore, the two-hole–one-particle final state $(4d^{-2}4f)$ level is expected to be shifted approximately the same as that of the single $4p$ hole level. Because the $4f$ electron is localized in the $4d$ hole region, one may approximate this two-hole–one-particle level by the one-hole level for the atom-oxide energy shift. Then the "relative" energy positions of the $4p$ level and $(4d^{-2}4f)$ levels are expected to not be sensitive to a change of environment.

VII. CONCLUDING REMARKS

The $L\gamma_{2,3}$ XES spectrum of Ba was measured with a high-resolution double-crystal spectrometer. The overall shape of the spectrum is similar to the $4p$ XPS spectrum. The spectrum was interpreted in terms of the $4p$ spectral function. Level splittings of a $4p$ hole level due to strong configuration interaction between a $4p$ hole level and $4d^{-2}4f$ multiplet level are observed and calculated by using the Green's function method. For a description of the satellite structure, it is important to take into account the $4d^{-2}4f$ multiplet levels. This differs from the case of the elements Pd to Xe where the main ionic excitation strength lies in the continuum. For Ba the main ionic excitation strength is concentrated in the $(4d^{-1})_{av}(4d^{-1}4f^1P)$ level. Therefore, the spectrum can be essentially treated as a two-level problem. It would be interesting to perform the Green's function calculations which treat the multiplet structure of the $4d^{-2}4f$ level in a more rigorous way. We leave such a calculation to the future.

ACKNOWLEDGMENTS

One of the authors (M.O.) is grateful to K. Ohno and S. J. Henke for help during the course of this work. We would like to thank John W. Cooper for critical comments of the manuscript.

---

*Present address: Institut für Physikalische und Theoretische Chemie der Technischen Universität, Postfach 3329, D-3300 Braunschweig, West Germany.

[1]G. Wendin and M. Ohno, Phys. Scr. **14**, 148 (1976).
[2]G. Wendin, *Structure and Bonding* (Springer, Berlin, 1981), Vol. 45, p. 1, and references therein.
[3]L. S. Cederbaum, J. Schirmer, W. Domcke, and W. von Niessen, J. Phys. B **10**, L549 (1977).
[4]S. P. Kowalczyk, L. Ley, R. L. Martin, F. R. McFeely, and D. A. Shirley, Faraday Discuss. Chem. Soc. **60**, 7 (1975).
[5]U. Gelius, J. Electron Spectrosc. **5**, 985 (1974).
[6]M. Ohno, Phys. Scr. **21**, 589 (1980).
[7]M. Ohno, J. Phys. C **13**, 447 (1980).
[8]R. E. LaVilla, Phys. Rev. A **17**, 1018 (1978).
[9]M. Ohno and G. Wendin, Solid State Commun. **39**, 875 (1987).
[10]M. Ohno and J-M Mariot, J. Phys. **14**, L1133 (1981).
[11]M. Ohno and R. E. LaVilla, Phys. Rev. A **38**, 3479 (1988).
[12]For $(4d^{-1})_{av}(4d^{-1}4f^1P)$, the $4f$ electron is coupled to the $4d$ core hole in a ^1P total angular momentum state with an extra spectator $4d$ hole. The subscript "av" denotes spherical average. See Ref. 1 for a further detail account.
[13]R. D. Deslattes and B. Simson, Rev. Sci. Instrum. **37**, 753 (1966).
[14]R. D. Deslattes, E. G. Kessler, W. C. Sauder, and A. Henins, Ann. Phys. (N.Y.) **129**, 378 (1980).
[15]R. D. Deslattes, Rev. Sci. Instrum. **38**, 616 (1967).
[16]H. F. Beyer, R. D. Deslattes, F. Folkmann, and R. E. LaVilla, J. Phys. B **18**, 207 (1985).
[17]M. Ohno and G. Wendin, J. Phys. B **12**, 1305 (1979).
[18]P. Putila-Mäntylä, M. Ohno, and G. Graeffe, J. Phys. B **16**, 3503 (1983).
[19]M. H. Chen, B. Crasemann, and H. Mark, At. Data Nucl. Data Tables **24**, 13 (1979).
[20]S. Svensson, N. Mårtensson, E. Basilier, P. A. Malmquist, U. Gelius, and K. Siegbahn, Phys. Scr. **14**, 141 (1976).
[21]B. Johansson and N. Mårtensson, Phys. Rev. B **21**, 4427 (1980).